Abstract: In this study, the influence of substrate surface finish on scratch resistance and associated failure mechanisms is investigated in the case of a TiN-coated hardmetal. Three different surface finish conditions are studied: as-sintered (AS), ground (G), and mirror-like polished (P). For G conditioned samples, scratch tests are conducted both parallel and perpendicular to the direction of the grinding grooves. It is found that coated AS, G and P samples exhibit similar critical load for initial substrate exposure and the same brittle adhesive failure mode. However, the damage scenarios are different, i.e. the substrate exposure is discrete and localized to the scratch tracks for G samples while a more pronounced and continuous exposure is seen for AS and P ones. Aiming to understand the role played by the grinding-induced compressive residual stresses, the study is extended to coated systems where ground substrates are thermal annealed (for relieving stresses) before being ion etched and coated. It yielded lower critical loads and changes in the mechanisms for the scratch-related failure; the latter depending on the relative orientation between scratching and grinding directions.

October 24, 2014

Professor Alan Matthews , Editor-in-Chief
Surface and Coatings Technology
Dept. of Engineering Materials, University of Sheffield,
Sir Robert Hadfield Building, Mappin Street,
Sheffield, S1 3JD, England, UK

RE: "Substrate surface finish effects on scratch resistance and failure mechanisms of TiN-coated hardmetals",
by J. Yang, J. J. Roa, M. Odén, M.P. Johansson-Jõesaa, J. Esteve and L. Llanes

Dear Professor Matthews,

Please find attached electronic files corresponding to our contribution on influence of substrate surface finish on scratch response and induced failure modes for TiN-coated hardmetals, which we (all authors do agree to the submission of the manuscript) offer for publication in *Surface and Coatings Technology.*

I hope it is found satisfactory.

Sincerely yours,

Luis Llanes

Prof. Luis Llanes
Ph. # + 34-934011083
Fax # + 34-934016706
email: luis.miguel.llanes@upc.es

Barcelona, January 13, 2015

Editorial Office

REF: Ms Nº:

Dear Editor,

Thank you for your email of December 2 informing us about your positive consideration of the referred manuscript, upon the completion of minor revisions, for its publication in Surface and Coatings Technology. From the reports appended in your email, it seems that the three reviewers have read the paper very carefully. Please thank them for their care and criticism. As requested, we have considered the indicated comments, and the following is a list of our responses (and modifications):

Reviewer #1's comments:

- The authors are congratulated to an excellent paper. The topic on surface topographical effects is important in many tribological applications and not well understood. A paper that investigates this systematically and in detail like this paper is a most welcome contribution. The paper is well and clearly written, the figures are clear and include excellent microscopy images.
The reviewer has only one suggestion for improvement for the authors to consider. The measurements of residual stresses in the surfaces are a very interesting part of the work. However, the presentation of the data in table 2 and in the text is not clear enough for the reader to understand the locations in the various surfaces where these residual stresses occur. Here the addition of a sketch may be the best way to clarify this.

Regarding reviewer 1's suggestion for improvement of the manuscript, although it seems rational and suitable, we feel that an additional figure (sketch) in a paper including already 10 other Figures (and most of them with multiple captions) may go beyond the (not written) limit associated with space limitation.

And aiming to clarify locations in the various surfaces where residual stresses occur, text has been slightly modified (Within last paragraph in section 3.1):

… The coated G condition has a maximum compressive stress of about -1.0 GPa in the substrate surface (i.e. just at the coating-substrate interface). As expected, this value is one order of magnitude higher than those assessed for the coated AS and P conditions at similar substrate surface location, i.e. -0.2 and -0.1 GPa respectively. However, it should be noted that such residual stress level at the substrate surface for coated G specimen is lower (about half) than what we have recorded for the same hardmetal and grinding conditions in its uncoated state [38]….

Reviewer #2's comments:

The authors examine the effect of substrate roughness on the critical load of PVD-coated TiN thin films. In particular they study three systems: as-sintered, ground and polished. The residual stresses for ground specimens are an order of magnitude greater than that of as-sintered and polished specimens. Meanwhile, as-sintered specimens exhibit higher surface roughness values compared to ground and polished specimens. All three materials exhibited similar scratch critical loads and the scratch failure mode is recovery spallation, along the edges of the scratch track. Furthermore, FIB reveals that cohesive failure is followed by adhesive failure between the coating and the substrate. In the specific case of ground specimens, thermal annealing results in lower critical loads; meanwhile for the thermally annealed ground specimens tested in the direction perpendicular to the grinding direction, buckling spallation occurs as well as recovery spallation.

Major Comments:

(1) Several authors (Steinmann et. al., Thin Sol. Film., 1987; Bromark et. al., Surf. & Coat. Technol. 1992) have reported that the adhesion of hard coatings decreases with the substrate surface roughness, which is in agreement with the authors findings. Nevertheless, the authors should provide the (Normal force, scratch path) curves and the (normal force, acoustic emission) curves and, if possible, overlay them with the scratch groove images for the sake of clarity.

In our study, different surface roughness values are also associated with distinctly different residual stress states in the substrate subsurface as well as different machining-induced damage (particularly regarding ground (G) surface finish conditions). Thus, our results are not directly comparable with the referred literature. As a result we do not assess any clear dependence of the critical load on substrate surface roughness, as also stated in the summary by Reviewer #2: "... *Meanwhile, as-sintered specimens exhibit higher surface*

roughness values compared to ground and polished specimens. All three materials exhibited similar scratch critical loads and the scratch failure mode is recovery spallation, along the edges of the scratch track..." (??)

We do have the data for plotting the requested curves but we do not see that they provide any additional useful information to the understanding of the results presented. In addition, the length of the scratch grooves is much smaller than the scratch track and sliding distance (as it may be seen in Figures 3, 4, 7 and/or 8). To provide the requested overlays would therefore require additional figures and corresponding text and consequently extend the length of the paper with basically no content gain. For the sake of clarity we have made no changes to manuscript regarding this item.

(2) The authors report that the hardness values measured via nano-indentation is invariant with the surface finish. The authors should provide more details regarding their testing procedure (force history,. Maximum load, loading rate,..). Moreover their finding seems a bit unlikely given the significant roughness of some of their specimens (450 nm for as-sintered specimens), which would require deep indentation tests (as a rule of thumb, the maximum penetration depth should be 5 times greater than the roughness of the sample and an order of magnitude less than the thickness of the coating). On the other hand, deep nano-indentations (1.8 micrometer for as-sintered specimens if we apply the criterion given) would generate a lot of plastic deformation and even lead to a composite coating-substrate response.

Reviewer #2 is completely right about this statement, and our writing should be blamed for the unintended confusion. Coating hardness was measured for all the coated surface conditions using similar testing variables. However, before doing so, and aiming to avoid roughness artifacts, all coatings were gently polished before nanoindentation testing. Accordingly, surface roughness for all the specimens was reduced and homogenized for all coated specimens. Information on this polishing pretreatment before nanoindentation testing has been added to the document as well as additional information on the testing procedure itself, as following (within the second paragraph in section 2):

Prior to nanoindentation testing all coatings were polished using a silica colloidal suspension in order to minimize the influence from surface roughness on the obtained hardness. The indents were positioned in a 4 by 4 matrix with a closest distance between two indents of 50 μm. Each indent was made to a maximum penetration depth of 2000 nm or until reaching maximum applied load of the equipment, i.e. 650 mN. This procedure ensures no overlapping effect from neighboring indents. The recorded load-displacement curves were evaluated for hardness by assuming a constant Poisson ratio of 0.25 [24] and using the method proposed by Oliver and Pharr [25]. The reported hardness is an averaged value from at least 12 indents. The shape of the diamond Berkovich indenter was calibrated for true penetration depths using a fused silica samples with known elastic modulus (72 GPa).

(3) The effect of heat treatment on ground specimens is puzzling. Typically, high residual compressive stresses in the coating lead to lower critical loads (Jindal et. al., Thin Sol. Films, 1987) and if we compare the ground specimens with the as-sintered and polished ones, this trend is verified. Following this line of thought, thermal annealing of ground specimens should yield higher critical loads. Another explanation for the low critical loads of thermally annealed ground specimens as well as the observed buckle propagation at the interface would be a more ductile substrate, which resembles the mechanism postulated by the authors. Nevertheless, for the sake of rigor, the authors should provide the hardness values of the initial ground substrate versus the ground and thermally annealed substrate

We agree with the referee that it would be nice to determine the mechanical properties locally in the first few microns below the interface in the WC/Co composite. However, obtaining such data cannot be done with any instrumentation we know, such that it makes sense when comparing it to the measured residual stress.

The stress is measured in the first 2 microns in depth but over an area of several square millimeters. Depth wise this is just a subsurface layer of microstructural length-scale, and we know that below this depth a very steep stress gradient exists, see for example ref 38. If we were to make indents that only extract samples' hardness from the first 2 micron we should do it with maximum 200 nm deep indents. Given the surface roughness and the heterogeneous microstructure the sought effect of residual stress relief would be completely lost in the data scatter.

We also want to point out that annealing was performed prior to coating deposition, i.e. the stress in the coating is not affected by the heat treatment.

Given that it is impossible to properly assess the mechanical state in the near surface region experimentally and that the coatings deposited are the same, we find our discussion regarding residual stress relief and an apparent substrate surface softening adequate and appropriate.

(4) In page 10 of the manuscript, the authors claim that the high compressive residual stresses and the mechanical performance of the substrate (that exhibits high values of stiffness and hardness) are at the origin of the observed scratch response. However by cross-referencing the reported failure modes, recovery and buckling spallation, with Bull's classification (Bull, Surf & Coat. Technol. 1991), we found an alternative explanation: poor bonding at the substrate/coating interface. The authors need to comment on the film/substrate interfacial strength and on how it could be improved.

We find this comment strange. The critical load for initial substrate exposure is about 100 N (i.e. an "outstanding scratch response"), which never can be considered as poor coating/substrate adhesion.

Minor Comments
(1) The authors should mention the ASTM standard C 1624- 05 as they are using this method to characterize the adhesion strength and failure modes of their specimens

We do not understand this comment as ASTM Standard C1624-05 is given as Ref. [30].

(2) Page 8: the sentence "The P specimen deviates from this trend since the ion-bombardment actually increases the roughness of the mirror polished surface." Is unclear. The trend mentioned in the sentence before is systematically satisfied by the Polished specimens.

Reviewer is right. Referred sentence has been removed from the text.

(3) In Figure 1, the authors should identify the "droplets" or "grove-like" features that are mentioned in Page 8.

Figure 1 has been slightly modified: "droplets" are now indicated by white arrows, whereas ""grove-like" features are identified by describing them (Figure's legend) in terms of the grinding direction (indicated by an external black arrow).
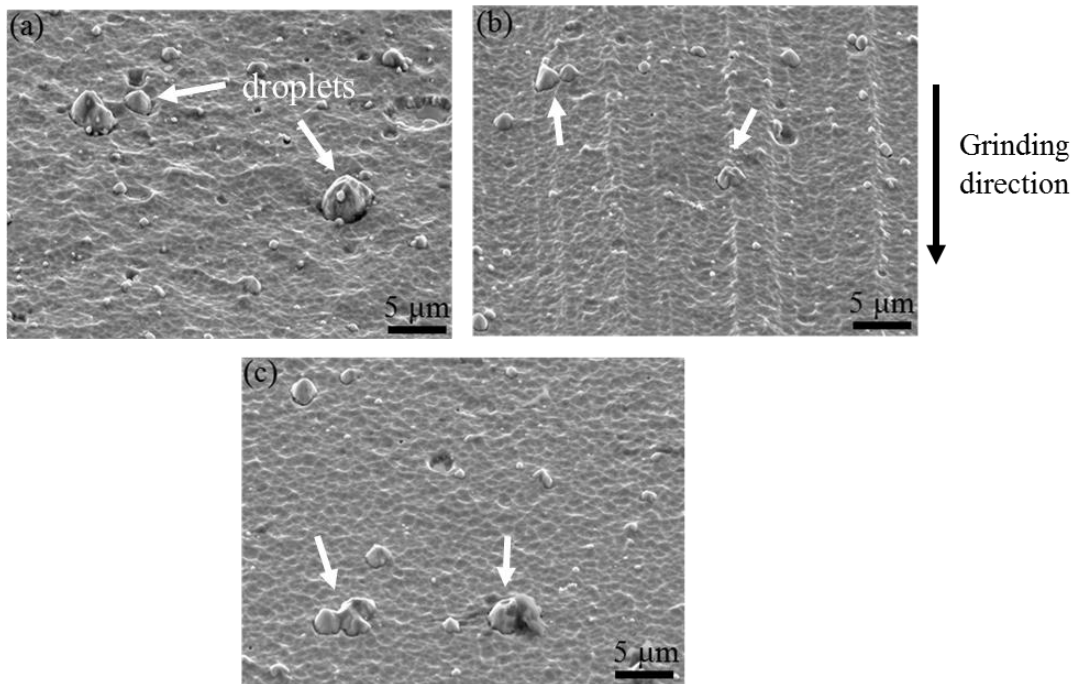
Fig. 1. Surface morphology of the coated systems resulting from different substrate surface finish: (a) AS, (b) G, and (c) P. Droplets are indicated by arrows, and surface texture is apparent in the G variant, which displays grove-like features following the grinding direction.

(4) Page 9: the authors claim that the residual stress in as-sintered specimens is not affected by the coating process. Unless the authors provide values of the residual stress before coating, this remains a non-proven claim.

Reviewer is right. Information on values of residual stresses at the AS substrate surface before coating has been included in the text.

Within last paragraph in section 3.1:

"… of the corresponding coated tools. The residual stress in the coated AS condition is within the experimental scatter of the value determined at the AS substrate surface before any ion-etching or coating, i.e. -123±12 MPa. Accordingly, it may be considered …

(5) Page 11, the authors vaguely outlined an alternative means to evaluate the critical load. This is a good point given that there the critical load as defined by the ASTM standard C 1624-05, that the authors seem to follow, is still the topic of significant controversy in the tribology community. Nevertheless, the authors should be more quantitative, specific and rigorous in identifying an alternative.

A simple image analysis of scratch tracks shown in Figure 4 would suggest that percentage of substrate exposure above 10-20% would already point out a ranking where G condition outperforms AS and P ones. However, a proposed alternative to evaluate critical load (to those commonly used: early exposure, 50% substrate exposure, etc.) requires a more extensive, quantitative study than the one here presented. Furthermore, the fact that interfacial strength for the investigated coating/substrate system is rather high, adds an experimental difficulty as scratch testing up to higher loads (aimed to induce further substrate exposure) was not attempted in order to avoid damage of spherical probes.

Reviewer #3's comments:

- An impressive piece of work! I recommend acceptance subject to a few minor points:-

As it was also the case regarding comments from Reviewer #1, we are really thankful to the positive general assessment from Reviewer 3!
Concerning reviewer 3's few minor points, our response is detailed below.

It would be useful to double-check the radius of the spherical probe. Often - eg as found in EU projects such as FASTE, it's found that the real geometry deviates from quoted at shallow depths. If the probe is well used I might expect R > 200um and this is a key factor in why you get Lc > 100. I know some coating manufacturers don't run their tests past 60 or 90 N to protect their diamonds.

Yes, we checked for radius changes of spherical probes, although usually after three tests. Several probes were employed throughout the investigation, all of them being double-checked to a radius of about 200 micron. No relevant difference was measured in critical load for initial coating detachment as whether "new" or "used" probes were used.

In the highlights, it's fairly well known that orientation vs scratch direction influences Lc - eg see the study by Larsson et al in Surf Eng and more recently at the nano- scale (eg Beake/Shi/Sullivan, in Tribology 5 (2011) 141). The possibly interesting thing is that the magnitude of the difference you found was less. It might be interesting to discuss why.

Although we understand Reviewer 3's viewpoint in this comment, it should be emphasized that our highlight on "different" scratch response refers to "mechanisms for the scratch-related failure" and not to L_c. Regarding the latter, as the Reviewer 3 has commented differences are rather minor. However, to compare them to those reported in the references indicated by the reviewer may be misleading. In the first case (Beake's paper), it must be noticed that studies are conducted at much lower length scales (nanocratch); thus, interaction between surface texture and scratch response is indeed quite different to that obtained in this investigation that has been focused in the "microscratch" regime. In the second case (Larsson's paper), critical load is defined on the basis of different (the first observed) failure mode: cohesive at the coating level in the transverse orientation vs adhesive in the longitudinal one. It clearly is not our case, where critical load is defined on the basis of one single mode: adhesive failure. Hence, comparison of relative differences between findings reported in both studies is not trivial either. Following the above ideas, and for the sake of clarity of the readers, we have not included the commented comparisons in the final version.

Is it normal to discuss Ry as max profile depth? Would be it better to describe it as a max surface height?

We agree with the referee and have modified Ry description to "maximum profile height".

We hope the modified version will now be completely suitable for publication. Once again, thank you for your time and cooperation.

Sincerely yours,

Luis Llanes

- ➢ Scratch-induced damage scenario is clearly dependent on surface finish condition.
- ➢ Adhesive failure in ground substrates is related to compressive residual stresses.
- ➢ Scratch response depends on relative scratch – grinding groove orientations.

Substrate surface finish effects on scratch resistance
and failure mechanisms of TiN-coated hardmetals

J. Yang[1,2], J. J. Roa[1,3], M. Odén[2], M.P. Johansson-Jõesaar[2,4],
J. Esteve[5] and L. Llanes*[1,3]

[1] CIEFMA - Departament de Ciència dels Materials i Engenyeria Metallúrgica, ETSEIB, Universitat Politècnica de Catalunya, Barcelona 08028, Spain
[2] Nanostructured Materials, Department of Physics, Chemistry, and Biology (IFM), Linköping University, Linköping 58183, Sweden
[3] CRnE – Center for Research on Nanoengineering, Universitat Politècnica de Catalunya, Barcelona 08028, Spain
[4] SECO Tools AB, Fagersta 73782, Sweden
[5] Departament de Física Aplicada i Òptica, Universitat de Barcelona, Barcelona 08028, Spain
* Corresponding author: luis.miguel.llanes@upc.edu

Abstract

In this study, the influence of substrate surface finish on scratch resistance and associated failure mechanisms is investigated in the case of a TiN-coated hardmetal. Three different surface finish conditions are studied: as-sintered (AS), ground (G), and mirror-like polished (P). For G conditioned samples, scratch tests are conducted both parallel and perpendicular to the direction of the grinding grooves. It is found that coated AS, G and P samples exhibit similar critical load for initial substrate exposure and the same brittle adhesive failure mode. However, the damage scenarios are different, i.e. the substrate exposure is discrete and localized to the scratch tracks for G samples while a more pronounced and continuous exposure is seen for AS and P ones. Aiming to understand the role played by the grinding-induced compressive residual stresses, the study is extended to coated systems where ground substrates are thermal annealed (for relieving stresses) before being ion etched and coated. It yielded lower critical loads and changes in the mechanisms for the scratch-related failure; the latter depending on the relative orientation between scratching and grinding directions.

Keywords: Scratch resistance; substrate surface finish; grinding; coated hardmetal; scratch failure mechanisms

1. Introduction

Physical vapor deposition (PVD) of hard coatings is a well-established surface modification route to increase the lifetime of cutting tools. The main reasons for the enhanced performance associated with hard coating deposition in terms of improved protection against mechanical and thermal loads are a lower friction and interaction between the tool and chip, and higher wear resistance across a wide range of cutting temperatures [1]. However, the tribological and mechanical behavior of coated tools depends not only on intrinsic properties of the deposited film but also on substrate surface and subsurface properties – such as topography and residual stress state – as well as on interface adhesion strength (e.g. Refs. [1-6]). It is particularly true in the case of coated tools based on WC-Co cemented carbides (backbone materials of the tool manufacturing industry and simply referred to as hardmetals in practice) as substrates. Similar to the case for other hard and brittle materials (e.g. structural ceramics [7]), geometry and/or close tolerances prescribed by the design of hardmetal tools are primarily attained by means of diamond grinding [8]. As a result of this abrasive machining route, mechanical- and thermal-induced alterations are introduced at both surface and subsurface levels [9-13], which may cause changes in the intrinsic cohesive strength of the substrate and the adhesion strength of the coating/substrate interface. Despite their importance, studies of surface integrity evolution throughout the different stages of the hardmetal coating process are scarce [6, 14, 15]; and knowledge on how it may affect the adhesion strength of the coated tools is even more limited. Such information is critical for further development and improved design of coated hardmetal tools for cutting applications.

In assessing the strength of a coated interface system, the scratch test is the most common method among the options described in the literature, e.g. Ref. [16]. The test is conducted such that a diamond indenter with a tip radius of between 100 and 500 μm slides over the coated surface with an increasing normal load typically between 1 to 200 N. In this context, "practical (extrinsic) adhesion" strength is evaluated in terms of critical forces associated with defined failure events. This is different from the fundamental adhesion strength which is ascribed to the bonding between coating and substrate. However, care must be taken on the quantitative analysis of the results (critical normal forces), as they are affected by various intrinsic and extrinsic parameters [17]. On the other hand, scratch testing is usually complemented by *in-situ* and post-

failure inspection of the failure mode evolution and involved mechanisms as a function of the applied load [18, 19]. Such studies have proven to be extremely useful for understanding the tribomechanical response of coated systems when subjected to sliding contacts. The individual influence of diverse factors such as the chemical nature of the contact, the hardness of both coating and substrate, and coating thickness may be separated. Recently, Sveen and coworkers used scratch testing to pinpoint the coating failure mechanisms on different hard materials used as substrate, i.e. high speed steel, cemented carbide or polycrystalline cubic boron nitride [20].

The main goal of this study was to investigate the influence of substrate surface finish on the scratch resistance and associated failure mechanisms for a TiN-coated WC-13wt%Co hardmetal prepared with three different surface finish conditions: as-sintered, ground, and mirror-like polished. The sliding contact response of the coated systems was evaluated by the scratch test technique and characterized by focused ion beam / field emission scanning electron microscopy (FIB/FESEM) with respect to surface morphology, subsurface damage and effective residual stress state.

2. Materials and Methods

A fine-grained hardmetal grade (WC-13wt%Co) was used as substrate material in this study. It was supplied as rectangular bars with 4×4×53 mm dimensions. Vickers hardness and Palmqvist fracture toughness values for the cemented carbide under consideration were 14.8 GPa and 11.2 MPa√m [21], both within the range of those usually reported in the literature for WC-Co hardmetals with similar binder content and carbide grain size (e.g. Refs. [22, 23]).

Three different surface finish conditions (on the 4×53 longitudinal section) prior to coating deposition were investigated: (i) as-sintered (AS), (ii) ground (G), and (iii) mirror-like polished (P). Plane surface grinding was performed using a commercial diamond abrasive wheel and coolant, the latter for preventing heat generation. On the other hand, polishing was sequentially done using diamond-containing disks, diamond suspensions until 3 μm, and a final step with a suspension of 45 nm colloidal silica particles. The TiN coating was deposited by means of an industrial reactive cathodic arc evaporation system MZR323. The deposition was performed

from pure Ti cathodes in a N_2 atmosphere at a pressure of 2 Pa. A substrate bias of -50 V was used to accelerate the Ti-ions towards the substrate and the temperature was maintained at 450 °C. Before deposition, the substrates were cleaned in ultrasonic baths of an alkali solution and alcohol. The system was evacuated to a pressure of less than 2.0 x 10^{-3} Pa, after which the substrates were sputter cleaned with about 500 eV Ar ions. All the substrates with the three surface finish conditions were mounted at the same height with respect to the cathodes on a rotating cylinder such that they all were deposited with the same (~ 3 μm) thick TiN coating in one deposition run.

Intrinsic hardness of deposited coatings was determined by nanoindentation (MTS Nanoindenter XP). Prior to nanoindentation testing all coatings were polished using a silica colloidal suspension in order to minimize the influence from surface roughness on the obtained hardness. The indents were positioned in a 4 by 4 matrix with a closest distance between two indents of 50 μm. Each indent was made to a maximum penetration depth of 2000 nm or until reaching maximum applied load of the equipment, i.e. 650 mN. This procedure ensures no overlapping effect from neighboring indents. The recorded load-displacement curves were evaluated for hardness by assuming a constant Poisson ratio of 0.25 [24] and using the method proposed by Oliver and Pharr [25]. The reported hardness is an averaged value from at least 12 indents. The shape of the diamond Berkovich indenter was calibrated for true penetration depths using a fused silica samples with known elastic modulus (72 GPa).

The surface integrity for each of the selected surface pretreatment conditions was characterized in terms of an assessment of the surface roughness and surface residual stress levels, as well as damage inspection. The surface roughness was measured by employing a stylus type, surface texture measuring system (Model Surftest SV512, Mitutoyo). Five measurements were performed per sample while the roughness parameters R_a (arithmetic deviation from the mean line through the complete profile) and R_y (maximum profile height) were recorded. For each surface finish variant, roughness data were gathered for the uncoated, the ion-etched and the ion-etched plus coated hardmetal substrates.

Surface residual stresses were determined by X-ray diffraction (XRD) with a Panalytical Empyrean four-circle diffractometer using a Cu-K_α radiation in a point focus mode using the $\sin^2\psi$ method. For the hardmetal substrate, only the WC phase was used for the residual stress assessment. Measurements were performed on the WC 211 reflection with a peak position of 2θ

~ 117° and the TiN 220 reflection with a peak position of 2θ ~ 61.3°, for the WC and TiN respectively [26]. Data was obtained using the side inclination technique (ψ-geometry) with 4-8 ψ-angles between 0 and 57°. The scattering data was fitted by either a Gauss or a Pseudo-Voigt function and residual stress value was then calculated by applying the $\sin^2\psi$-d method using X-ray elastic constants for the WC 211 (v=0.2 and E=491GPa) and TiN 220 (v=0.2 and E=491GPa) [26]. At this stage, it should be pointed out that the recorded residual stress values are also affected, in addition to the surface finish, by intrinsic factors caused by for example differences in coefficients of thermal expansion between WC and the metallic binder, i.e. sintering at high temperatures and subsequent cooling generates residual microstresses. According to literature reports based on both XRD and neutron diffraction techniques [27-29], residual stress values in the range from -100 to -500 MPa are expected in the WC phase when machining-induced effects can be disregarded.

Scratch tests were performed by drawing a Rockwell C diamond stylus (with a tip radius of 200 μm) across the sample surface under linearly increasing load, from 5 to 120 N (150 N for the coated P system), at a loading rate of 100 N/min [30]. During the scratch test, friction force and acoustic emission (AE) signals were continuously recorded. For G conditioned specimens, scratch tests were conducted both parallel (G-//) as well as perpendicular (G-⊥) to the grinding groove direction. Critical normal load (L_c) was defined as the load value corresponding to initial substrate exposure, and it was determined by direct inspection of the scratch track through optical microscopy and by the AE system. Evolution of damage induced by scratch and the associated failure mechanisms were examined by means of FESEM (JEOL JSM-7001F). Subsurface damage at the location of critical load was evaluated through FESEM imaging of FIB-prepared cross-sections using a dual beam Workstation (Zeiss Neon 40).

3. Results and Discussion

3.1 Surface integrity characterization: roughness, subsurface damage and residual stresses

Roughness features for all the surface finish conditions studied are intimately related to the surface topography resulting from processing and subsequent machining. Mean and standard deviation values for roughness parameters R_a and R_y are given in **Table 1**. They are presented in terms of both substrate surface finish condition (AS, G and P) as well as stages within the PVD coating process chain (uncoated, ion-etched and coated). It is clear that grinding and polishing increasingly reduce the relatively high initial roughness values exhibited by the AS sample. Similar trends are observed for ion-cleaned surfaces, but here the relative changes are less pronounced. ~~The P specimen deviates from this trend since the ion bombardment actually increases the roughness of the mirror polished surface.~~ When the coating is deposited, roughness increases for all the studied conditions when compared to both uncoated and ion-etched conditions. The relative roughness increase is significant for the P-condition, reaching values similar to the ones of the coated G specimens. The high surface roughness in the coated conditions is due to droplets (indicated by arrows) in the TiN-coatings, see **Figure 1**. These microstructural heterogeneities, here of sizes up to several microns, are typical in films deposited by cathodic arc evaporation [31-35]. They are usually weakly bonded to the bulk coating and prompted to drop out from the surface under tribomechanical service conditions [34, 36, 37].

In addition to the referred droplets, surface texture is apparent in the G variant, which displays grove-like features following the grinding direction (**Figure 1**). Cross-sectional views attained through FIB milling (**Figure 2**) not only supports above observation but also highlights grinding-induced damage in terms of carbide microcracking, following either transgranular or intergranular (between contiguous carbide grains) paths, down to depths of approximately 0.5 μm (**Figure 2b**). Similar subsurface damage features are not discerned in the coated substrates with AS or P finish condition. The difference between the AS and P conditions in terms of roughness is inherited from the difference in substrate roughness. In **Figure 2** this is seen as a wavy substrate-coating interface, which is more pronounced for the AS condition. Our findings of grinding-induce damage are in accord with those reported by Hegeman et al. [8], and are the result of the applied stresses exerted by the diamond abrasive grains during machining. On the other hand, the relatively soft metal binder is smeared out over the surface with the pulverized WC grains and may be either partly removed from the surface together with WC grain fragments or redistributed at the subsurface level. Finally, cross-sectional inspection permits to observe that

deposited TiN coatings are dense and uniform, with fine-grained columns along the growth direction of their thickness.

The residual stresses recorded in the WC phase in the surface of coated substrates for the AS, G and P surface finish conditions are given in **Table 2**. The residual stress level for the TiN coating is also listed in this table. The coated G condition has a maximum compressive stress of about -1.0 GPa in the substrate surface (i.e. just at the coating-substrate interface). As expected, this value is one order of magnitude higher than those assessed for the coated AS and P conditions at similar substrate surface location, i.e. -0.2 and -0.1 GPa respectively. However, it should be noted that such residual stress level at the substrate surface for coated G specimen is lower (about half) than what we have recorded for the same hardmetal and grinding conditions in its uncoated state [38]. This difference is ascribed to thermal annealing effects during the coating process (ion cleaning and film deposition), which lead to partial relief of the grinding-induced residual stresses [6, 14, 15]. Nevertheless, the remnant stresses in the substrate surface after coating for the G specimen are still significant, and influences the tribomechanical performance of the corresponding coated tools. The residual stress in the coated AS condition is within the experimental scatter of the value determined at the AS substrate surface before any ion-etching or coating, i.e. -123±12 MPa. Accordingly, it may be considered as a reference level of the residual stress state of the hardmetal substrate and it is within the range of the residual stress values reported for the WC phase in cemented carbides after sintering [27-29]. Within this context, the fact that P and AS coated specimens exhibit similar residual stress values would sustain the description of the polishing being a gentle material removal procedure, such that no additional damage or stress are introduced.

3.2 Scratch resistance and failure mechanisms

In this investigation critical normal load (L_c) was defined as the load value corresponding to initial substrate exposure. It was determined by direct inspection of the scratch track through optical microscopy and an AE system. In general L_c values are high (above 80 N) for all the studied surface finish conditions (**Table 3**). Furthermore, they are relatively close to each other,

with L_c values for coated G specimens (particularly the G-$\perp$ orientation) showing a slight trend towards lower levels, as compared to coated AS and P specimens.

Before any substrate exposure, plastic deformation and localized cohesive failure (associated with the outgrowths from droplets in the coating surface) are the only deformation/failure mechanisms evidenced for all the cases (**Figure 3**). Cracking feature are scarce, even at 80 N, similar to what has been reported for other TiN/hardmetal systems [20, 39, 40]. For G-$\perp$ condition (**Figure 3b**), the coating inside the scratch track seems to display some fragmentations, as a result of the transversal interaction between the grinding grooves and the sliding diamond tip. The main reasons for the found outstanding scratch response are the elevated stiffness and hardness of the underlying hardmetal substrate as well as the relatively high intrinsic compressive stresses exhibited by the deposited coating. These two factors are both independent of the substrate surface finish condition.

Damage appearance and evolution (as related to substrate exposure) are shown for three particular load levels: 95 N, 110 N, and 120 N, in **Figure 4**. All the coated systems display local interfacial spallation along the scratch track, with bright areas corresponding to substrate exposure. This is a brittle failure mode, referred to as recovery spallation after Bull [18, 19]. It is associated with deformation recovery in the scratch track after passage of the diamond stylus. When the scratched region is unloaded, the elastic deformation in the coating and the substrate is relaxed. However, due to plastic deformation of the substrate, the elastic energy cannot be completely dissipated and residual strains remain. Such strains are instead relaxed by through-thickness cracking of the coating, converting any tensile recovery stress in the coating into shear stresses at the coating-substrate interface near these cracks. Propagation of these interfacial cracks may lead to spallation at either side of the scratch track [18, 19, 41].

Although all the studied coated systems exhibit similar critical load for initial substrate exposure and the same predominant failure mode (brittle – recovery spallation) when scratch tested, it is evident from **Figure 4** that the adhesive failure scenarios is different depending on substrate surface finish. Within this context, while the critical load shows a trend toward higher values for coated AS and P compared to G specimens, early and subsequent coating detachment is pronounced and continuous, particularly in the coated AS surface finish condition (**Figure 4a**). This is in contrast to the more discrete and localized damage features found in the scratch tracks

for the two coated G conditions. A difference can also be seen when comparing G-// and G-⊥, where the spalled regions along the scratch track are more elongated and continuous (higher aspect ratio) for G-// (**Figure 4c**). With this in mind, the qualitative analysis of the scratch tracks shown in **Figure 4** based on a definition of the critical load as the load for first substrate exposure may be misleading. If instead a definition for the critical load were based on reaching a certain percentage of substrate exposure - beyond early adhesive failure - a different ranking of the surface finish conditioning could result, where the coated G systems would outperform AS and P.

Figure 5 shows top and inclined views at locations along scratch track edges associated with L_c (early adhesive failure) for all the coated systems. FIB prepared cross-sections at these locations are presented in **Figure 6**. Interfacial cracking is always evidenced, an observation that highlights the adhesive failure nature of the recovery spallation mode identified above. Cohesive failure within the substrate is not observed for any specimen. Despite the presence of subsurface cracks in the G specimens inherited from the damage during grinding (arrows in **Figure 2b**), also these specimens fail at the film substrate interface. It emphasizes the importance of the grinding-induced compressive residual stresses existing in the substrate. Here they are large enough to prevent failure of the substrate and enhance the tribomechanical performance of the coated hardmetals.

Another noteworthy observation from **Figures 5** and **6** concerns the severe loss of mechanical integrity of the coating in the AS specimen. Although intercolumnar cracking is common to all the coated systems, failure scenario at the small length scale of the film is rather catastrophic for AS condition. It yields as a consequence the pronounced delamination found for this system as applied load increases from 95 to 120 N during the scratch test (**Figure 4a**). As this surface finish condition does not imply any machining-induce damage or residual stresses, the severe film cracking and crushing evidenced must then be directly associated with a stress-rising effect implicit to its pronounced interface waviness (**Table 1**).

3.3 Heat treatment of ground hardmetals (prior to TiN coating deposition): influence on scratch resistance and failure mechanisms

Following the ideas presented and discussed in the previous section, it is clear that the scratch response for coated G specimens results from the combined effect of the stress state (including the compressive residual component assessed), surface topography (depending on orientation of grinding grooves) and induced damage in the substrate at both surface (effective interface) and subsurface levels. Within this context, the observation of adhesive failure is an interesting finding as it indirectly underlines the relevance of the compressive residual stresses for inhibiting cohesive failure within the substrate. In order to provide a direct proof of the above statement, the scratch resistance and associated failure mechanisms are evaluated for coated G specimens where the grinding-induced residual stresses are removed. This is done with a heat treatment of the ground substrates such that no additional changes of the other variables, i.e. surface topography and surface/subsurface damage, are introduced. In this regard, high temperature annealing of hardmetals has been validated as a successful protocol for relieving residual stresses, independent of nature (tensile/compressive) or source (mechanical abrasion [38, 42, 43] or electrical discharge machining [44-46]). Here it is used a heat treatment at 920 °C for 1 h in vacuum of ground hardmetal substrates before TiN deposition. The resulting specimens are here referred to as GTT. The residual stress state for these GTT samples decreased to about -0.1 GPa, while surface/subsurface damage remained unchanged [38].

Scratch tests were carried on coated GTT systems, both transversely (GTT-⊥) and parallel (GTT-//) to the orientation of grinding grooves. Critical loads corresponding to early substrate exposure for GTT-⊥ and GTT-// were found to be 76 ± 6 N and 87 ± 2 N respectively. It should be noted that not only L_c values are about 10% lower than those determined for G-⊥ and G-//, but also initial substrate exposure is more defined in the heat treated specimens, particularly for the GTT-⊥ condition (**Figure 7**).

Detailed views of scratch tracks for GTT-⊥ and GTT-// specimens are shown in **Figure 8**. Direct comparison of the failure mechanisms between G and GTT samples (using **Figure 4** as reference) yields that GTT-⊥ shows more pronounced recovery spallation and buckling failure than G-⊥. On the other hand, the differences between GTT-// and G-// specimens are less significant. The only difference observed is an indication of a more extended coating detachment along track edges for the heat treated (prior to coating) specimen.

Different from the recovery spallation failure mode, buckling is a less intense failure mode usually confined within the scratch track [18]. It generally occurs ahead of the moving indenter, with coating detachment being enhanced by the pile up of substrate material ahead of the stylus. As the chemical nature of the hardmetal substrate for both GTT-⊥ and G-⊥ coated systems is the same, the emergence of buckling cracking and spallation within the scratch track must then be associated with an effectively lower hardness and stiffness of the heat treated substrate at the subsurface level, still damaged but without the load-bearing support provided by compressive residual stresses. However, this would also be the case for GTT-//, and buckling was not seen for this condition. Thus, surface texture should also be invoked in the analysis in order to understand the additional failure mode in GTT-⊥. The surface waviness when oriented perpendicular to the direction of the stylus movement is likely to aid material flow such that pile-up occurs in front of the stylus. Such pile-up results in buckling generating cracks aligned to the existing grinding grooves in accord with our observations. The described damage scenario is further supported in **Figure 9**. It shows a FIB-milled longitudinal cross-section inside the scratch track where buckling-related damage first occurred (applied normal load about 65 N). The massive flow of the substrate is apparent in the form of a localized pile-up.

In order to evaluate if the failure related to substrate exposure occurred through adhesive or cohesive detachment, cross-sections were FIB-milled along the scratch track edges at locations corresponding to L_c for GTT-⊥ and GTT-// specimens (**Figure 10**). The failure mode is different for the two conditions. For GTT-⊥ interfacial delamination dominated (**Figure 10a and 10c**), yielding a failure scenario similar to the ones observed for AS, G-⊥, G-// and P systems. It emphasizes the good combination of mechanical properties, particularly in terms of fracture toughness to hardness ratio, exhibited by the hardmetal under consideration, as cohesive failure of a cracked, residual stress-free subsurface was still less prone than the observed adhesion one. Hence, tolerance to preexisting damage (directly related to fracture toughness) is here postulated as a critical microstructural design parameter for hard substrates, if cohesive fracture wants to be avoided [47]. If this is accomplished, as far as other material properties required for a given application are satisfied, the life of a coated hardmetal may be dramatically increased.

However, additional extrinsic factors such as surface texturing must also be included in the analysis. For example, the intrinsic parameters of the coating and substrate are not sufficient to

describe the behavior of the GTT-// system. **Figure 10b and 10d** shows cohesive failure just beneath the interface at the track edges of GTT-//. It is well known that different sets of crack patterns evolve during surface grinding: long semi-circular cracks parallel to the grinding marks and transverse cracks orthogonal to the referred marks [10, 11, 48]. Within this context, Subhash et al. [49] have observed in silicon nitride that for the same scratch depth or the same imposed force level, scratches parallel to the grinding direction result in greater damage than scratches conducted transverse to the grinding direction. Assuming a similar damage anisotropy also exist in ground hardmetals, the spallation scenario discerned in this study could be explained on the basis of favored interconnection (through subcritical propagation) of the discrete long flaws oriented parallel to the grinding grooves during scratch testing for the G-// and GTT-// systems. As a consequence, oriented and elongated substrate exposure - as related to longer flaws; and thus, higher probability of cohesive failure through the substrate - would be expected for coated G-// and GTT-// systems, as it is experimentally found.

Conclusions

The investigation of the influence of substrate surface finish on the scratch resistance and associated failure mechanisms of a TiN coated WC-13wt%Co hardmetal grade leads to the following main results:

(1) Independent of substrate surface finish under consideration, coated AS, G and P samples exhibit similar critical load for initial substrate exposure as well as same predominant failure mode (brittle – recovery spallation) as they get scratched. However, clear differences in the failure scenario were evidenced: pronounced and continuous substrate exposure for AS and P conditions, contrasting with rather discrete and quite localized damage features in the scratch tracks for the G samples.

(2) Interfacial cracking was found as the main scratch-induced failure mechanism for coated AS, G and P surface finish conditions. It highlights the adhesive failure nature of the recovery spallation mode identified along scratch track edges. On the other hand,

cohesive failure within the substrate was not evidenced even in the coated G systems, where substrates exhibit at the subsurface level localized damage inherited from early grinding.

(3) Relief of the grinding-induced compressive residual stresses (through high temperature annealing) results in lower critical loads for initial substrate exposure and changes in failure mechanisms (emergence of buckling cracks within scratch track for GTT-$\perp$ condition) and failure mode (cohesive through the substrate subsurface for GTT-// condition).

(4) Scratch response of ground and coated hardmetals is found to be dependent upon relative orientation between scratch and grinding directions. As scratches are conducted parallel to the grinding groove direction, substrate exposure becomes elongated and continuous and probability of cohesive damage along substrate subsurface increases.

Acknowledgements

References

[1] Bouzakis KD, Michailidis N, Skordaris G, Bouzakis E, Biermann D, M'Saoubi R. Cutting with coated tools: coating technologies, characterization methods and performance optimization. CIRP Annals - Manufacturing Technology. 2012;61:703-23.

[2] Bromark M, Larsson M, Hedenqvist P, Olsson M, Hogmark S. Influence of substrate surface topography on the critical normal force in scratch adhesion testing of TiN-coated steels. Surface and Coatings Technology. 1992;52:195-203.

[3] Tönshoff HK, Karpuschewski B, Mohlfeld A, Seegers H. Influence of subsurface properties on the adhesion strength of sputtered hard coatings. Surface and Coatings Technology. 1999;116–119:524-9.

[4] Byrne G, Dornfeld D, Denkena B. Advancing cutting technology. CIRP Annals - Manufacturing Technology. 2003;52:483-507.

[5] Casas B, Anglada M, Sarin VK, Llanes L. TiN coating on an electrical discharge machined WC-Co hardmetal: surface integrity effects on indentation adhesion response. Journal of Materials Science. 2006;41:5213-9.

[6] Denkena B, Breidenstein B. Influence of the residual stress state on cohesive damage of PVD-coated carbide cutting tools. Advanced Engineering Materials. 2008;10:613-6.

[7] Marinescu ID, Hans Kurt Tonshoff HK, Inaski I. Handbook of ceramic grinding and polishing. New York: Noyes Publications/William Andrew Publishing, L.L.C; 1998.

[8] Hegeman JBJW, De Hosson JTM, de With G. Grinding of WC–Co hardmetals. Wear. 2001;248:187-96.

[9] Saljé E, Moehlen H. Material removal in grinding of advanced ceramics. 3rd International Grinding Conference. Dearborn, MI, USA SME Technical Paper MR88-498, Society of Manufacturing Engineers; 1988.

[10] Li K, Warren Liao T. Surface/subsurface damage and the fracture strength of ground ceramics. Journal of Materials Processing Technology. 1996;57:207-20.

[11] Zhang B, Zheng XL, Tokura H, Yoshikawa M. Grinding induced damage in ceramics. Journal of Materials Processing Technology. 2003;132:353-64.

[12] Merkleina M, Andreasa K, Engela U. Influence of machining process on residual stresses in the surface of cemented carbides. Procedia Engineering. 2011;19:252-7.

[13] Jawahir IS, Brinksmeier E, M'Saoubi R, Aspinwall DK, Outeiro JC, Meyer D, et al. Surface integrity in material removal processes: Recent advances. CIRP Annals - Manufacturing Technology. 2011;60:603-26.

[14] Denkena B, Breidenstein B. Residual stress distribution in PVD-coated carbide cutting tools: Origin of cohesive damage. Tribology in Industry. 2012;34:158-65.

[15] Breidenstein B, Denkena B. Significance of residual stress in PVD-coated carbide cutting tools. CIRP Annals - Manufacturing Technology. 2013;62:67-70.

[16] Chen J, Bull SJ. Approaches to investigate delamination and interfacial toughness in coated systems: an overview. Journal of Physics D: Applied Physics. 2011; 44:1-35.

[17] Steinmann PA, Tardy Y, Hintermann HE. Adhesion testing by the scratch test method: The influence of intrinsic and extrinsic parameters on the critical load. Thin Solid Films. 1987;154:333-49.

[18] Bull SJ. Failure modes in scratch adhesion testing. Surface and Coatings Technology. 1991;50:25-32.

[19] Bull SJ. Failure mode maps in the thin film scratch adhesion test. Tribology International. 1997;30:491-8.

[20] Sveen S, Andersson JM, M'Saoubi R, Olsson M. Scratch adhesion characteristics of PVD TiAlN deposited on high speed steel, cemented carbide and PCBN substrates. Wear. 2013;308:133-41.

[21] Sheikh S, M'Saoubi R, Flasar P, Schwind M, Persson T, Yang J, et al. Fracture toughness of cemented carbides: Testing method and microstructural effects. International Journal of Refractory Metals and Hard Materials 2014; doi: 10.1016/j.ijrmhm.2014.08.018

[22] Shatov AV, Ponomarev SS, Firstov SA. Hardness and deformation of hardmetals at room temperature. In: Sarin VK, Mari D, Llanes L (Vol. eds.), *Comprehensive Hard Materials*. Elsevier 2014; Vol. 1, Ch. 1.09: p. 301–43.

[23] Shatov AV, Ponomarev SS, Firstov SA. Fracture and strength of hardmetals at room temperature. In: Sarin VK, Mari D, Llanes L (Vol. eds.), *Comprehensive Hard Materials*. Elsevier 2014; Vol. 1, Ch. 1.10: p. 345–62.

[24] Vijgen ROE, Dautzenberg JH. Mechanical measurement of the residual stress in thin PVD films. Thin Solid Films. 1995;270:264-9.

[25] Oliver WC, Pharr GM. An improved technique for determining hardness and elastic modulus using load and displacement sensing indentation experiments. Journal of Materials Research. 1992;7:1564-83.

[26] Eigenmann B, Macherauch E. Röntgenographische untersuchung von spannungszuständen in werkstoffen. Materialwissenschaft und Werkstofftechnik. 1996;27:11.

[27] Mari D, Krawitz AD, Richardson JW, Benoit W. Residual stress in WC-Co measured by neutron diffraction. Materials Science and Engineering: A. 1996;209:197-205.

[28] Larsson C, Odén M. X-ray diffraction determination of residual stresses in functionally graded WC–Co composites. International Journal of Refractory Metals and Hard Materials. 2004;22:177-84.

[29] Livescu V, Clausen B, Paggett JW, Krawitz AD, Drake EF, Bourke MAM. Measurement and modeling of room temperature co-deformation in WC–10 wt.% Co. Materials Science and Engineering: A. 2005;399:134-40.

[30] ASTM C 1624-05: Standard test method for adhesion strength and mechanical failure modes of ceramic coatings by quantitative single point scratch testing. ASTM International Standards, USA, 2005.

[31] Matthews A, Lefkow AR. Problems in the physical vapour deposition of titanium nitride. Thin Solid Films. 1985; 126:283-91.

[32] Münz WD, Lewis DB, Creasey S, Hurkmans T, Trinh T, Ijzendorn W. Defects in TiN and TiAlN coatings grown by combined cathodic arc/unbalanced magnetron technology. Vacuum. 1995;46:323-30.

[33] Anders A. Approaches to rid cathodic arc plasmas of macro- and nanoparticles: a review. Surface and Coatings Technology. 1999;120–121:319-30.

[34] Harlin P, Carlsson P, Bexell U, Olsson M. Influence of surface roughness of PVD coatings on tribological performance in sliding contacts. Surface and Coatings Technology. 2006;201:4253-9.

[35] Mubarak A, Hamzah E, Toff MRM. Study of macrodroplet and growth mechanisms with and without ion etchings on the properties of TiN coatings deposited on HSS using cathodic arc physical vapour deposition technique. Materials Science and Engineering: A. 2008;474:236-42.

[36] Carvalho NJM, Zoestbergen E, Kooi BJ, De Hosson JTM. Stress analysis and microstructure of PVD monolayer TiN and multilayer TiN/(Ti,Al)N coatings. Thin Solid Films. 2003;429:179-89.

[37] Ramírez G, Mestra A, Casas B, Valls I, Martínez R, Bueno R, et al. Influence of substrate microstructure on the contact fatigue strength of coated cold-work tool steels. Surface and Coatings Technology. 2012;206:3069-81.

[38] Yang J, Odén M, Johansson-Jõesaar MP, Llanes L. Grinding effects on surface integrity and mechanical strength of WC-Co cemented carbides. Procedia CIRP. 2014;13:257-63.

[39] Nordin M, Larsson M, Hogmark S. Mechanical and tribological properties of multilayered PVD TiN/CrN. Wear. 1999;232:221-5.

[40] Casas B, Wiklund U, Hogmark S, Llanes L. Adhesion and abrasive wear resistance of TiN deposited on electrical discharge machined WC-Co cemented carbides. Wear. 2008;265:490-6.

[41] Bull SJ, Berasetegui EG. An overview of the potential of quantitative coating adhesion measurement by scratch testing. Tribology International. 2006;39:99-114.

[42] Exner HE. The influence of sample preparation on Palmqvist's method for toughness testing of cemented carbides. Transactions of the Metallurgical Society of AIME 1969; 245: 677-83.

[43] Torres Y, Casellas D, Anglada M, Llanes L. Fracture toughness evaluation of hardmetals: influence of testing procedure. International Journal of Refractory Metals & Hard Materials. 2001; 19:27-34.

[44] Casas B, Lousa A, Calderón J, Anglada M, Esteve J, Llanes L. Mechanical strength improvement of electrical discharge machined cemented carbides through PVD (TiN, TiAlN) coatings. Thin Solid Films. 2004;447–448:258-63.

[45] Casas B, Torres Y, Llanes L. Fracture and fatigue behavior of electrical-discharge machined cemented carbides. International Journal of Refractory Metals & Hard Materials. 2006;24:162-7.

[46] Llanes L, Casas B, Torres Y, Salán N, Mestra A. Fatigue performance improvement of electrical discharge machined hardmetals by means of combined thermal annealing and surface modification routes. International Journal of Refractory Metals and Hard Materials. 2013;36:60-5.

[47] Góez A, Coureaux D, Ingebrand A, Reig B, Tarrés E, Mestra A, et al. Contact damage and residual strength in hardmetals. International Journal of Refractory Metals and Hard Materials. 2012;30:121-7.

[48] Marshall DB, Evans AG, Khuri Yakub BT, Tien JW, Kino GS. The nature of machining damage in brittle materials. Proceedings of the Royal Society: A. 1983;385:461-75.

[49] Subhash G, Marszalek MA, Maiti S. Sensitivity of scratch resistance to grinding-induced damage anisotropy in silicon nitride. Journal of the American Ceramic Society. 2006;89:2528-36.

List of Tables and Figures

Table 1.

Table 1. Nomenclature and roughness parameters (R_a and R_y) associated with substrate surface conditions and the coating process steps: uncoated; ion-etched; and coated

Condition	Substrate surface finish	R_a (μm)			R_y (μm)		
		Uncoated	Ion-etched	Coated	Uncoated	Ion-etched	Coated
AS	As-sintered	0.37±0.10	0.36±0.08	0.45±0.08	2.73±0.76	2.34±0.44	2.95±0.55
G	Ground	0.20±0.07	0.16±0.02	0.25±0.05	1.05±0.35	1.03±0.12	1.72±0.30
P	Polished	0.01±0.01	0.09±0.01	0.27±0.05	0.11±0.04	0.59±0.06	1.54±0.20

Table 2.

Table 2. Residual stresses measured (for the WC phase) on the substrate surface of coated systems for the AS, G and P conditions. The intrinsic residual stresses level for the coating is also listed for comparison purpose.

Condition	Residual stresses (MPa)
AS+Coat	-157±13
G+Coat	-1071±24
P+Coat	-59±15
Coating	-3299±140

Table 3.

Table 3. Critical normal load L_c determined in the scratch test, corresponding to the initial substrate exposure. G-$\perp$ and G-// represent orthogonal and parallel scratches with respect to the grinding marks, respectively.

Condition	L_c (N)
AS	101±6
G-$\perp$	89±9
G-//	98±2
P	104±2
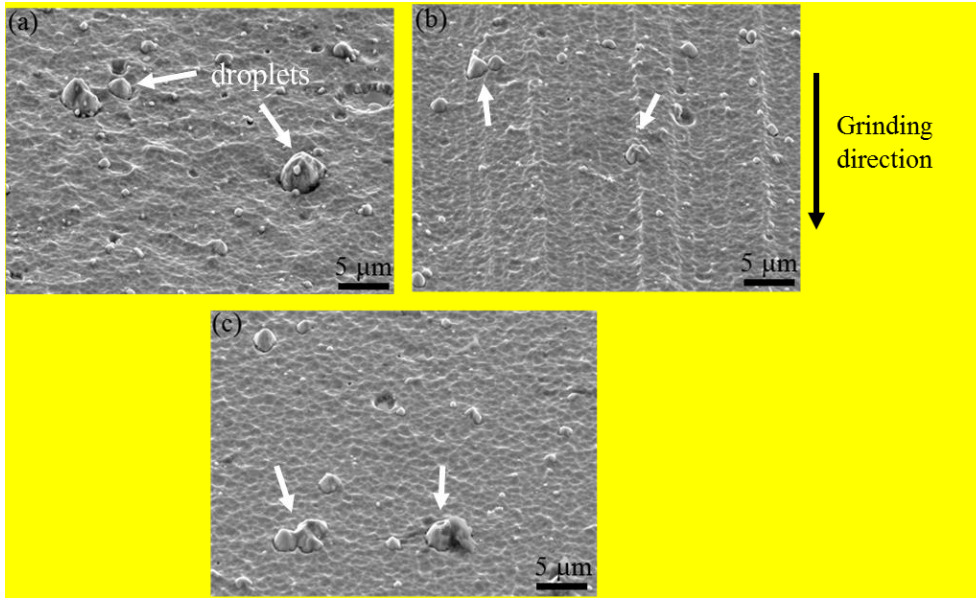
Fig. 1. Surface morphology of the coated systems resulting from different substrate surface finish: (a) AS, (b) G, and (c) P. Droplets are indicated by arrows, and surface texture is apparent in the G variant, which displays grove-like features following the grinding direction.

Figure 2.
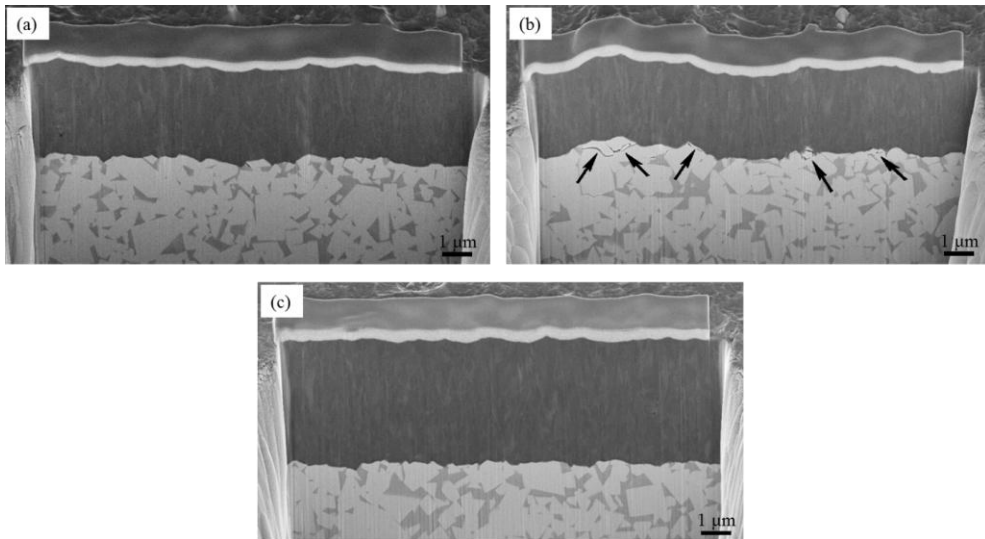
Fig. 2. Cross-section view of the coated systems resulting from different substrate surface finish: (a) AS, (b) G, and (c) P. Note that FIB milling was made perpendicular to the grinding marks, and grinding-induced damage are pointed out with arrows.

Figure 3.
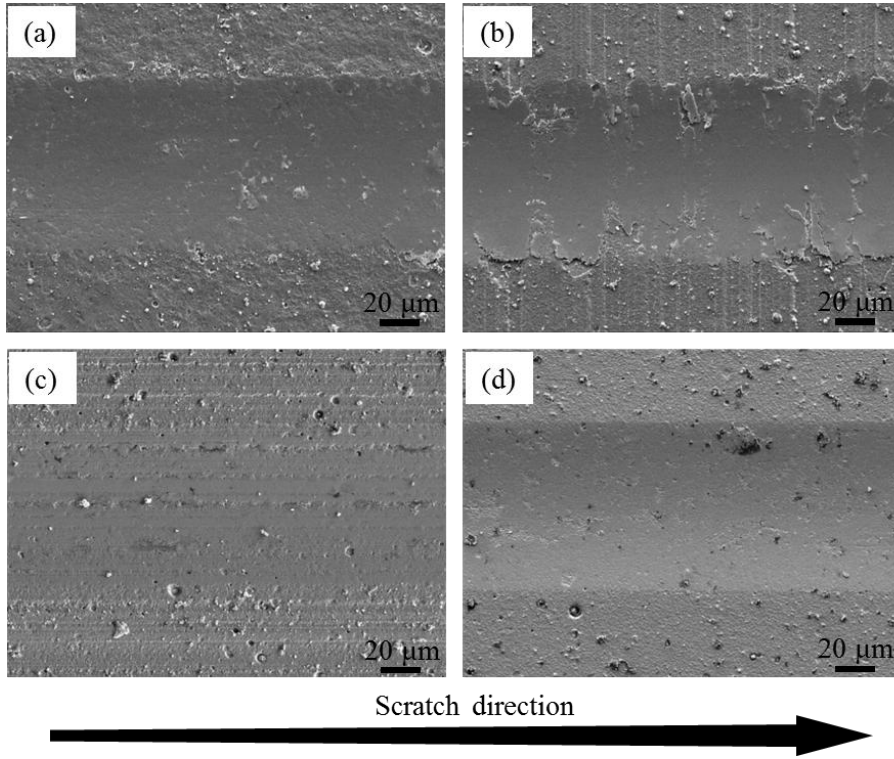
Scratch direction

Fig. 3. Scratch track view corresponding to an applied normal load of 80 N for each substrate surface finish condition: (a) AS; (b) G-⊥; (c) G-// and (d) P. Scratch direction from left to right.

Figure 4.
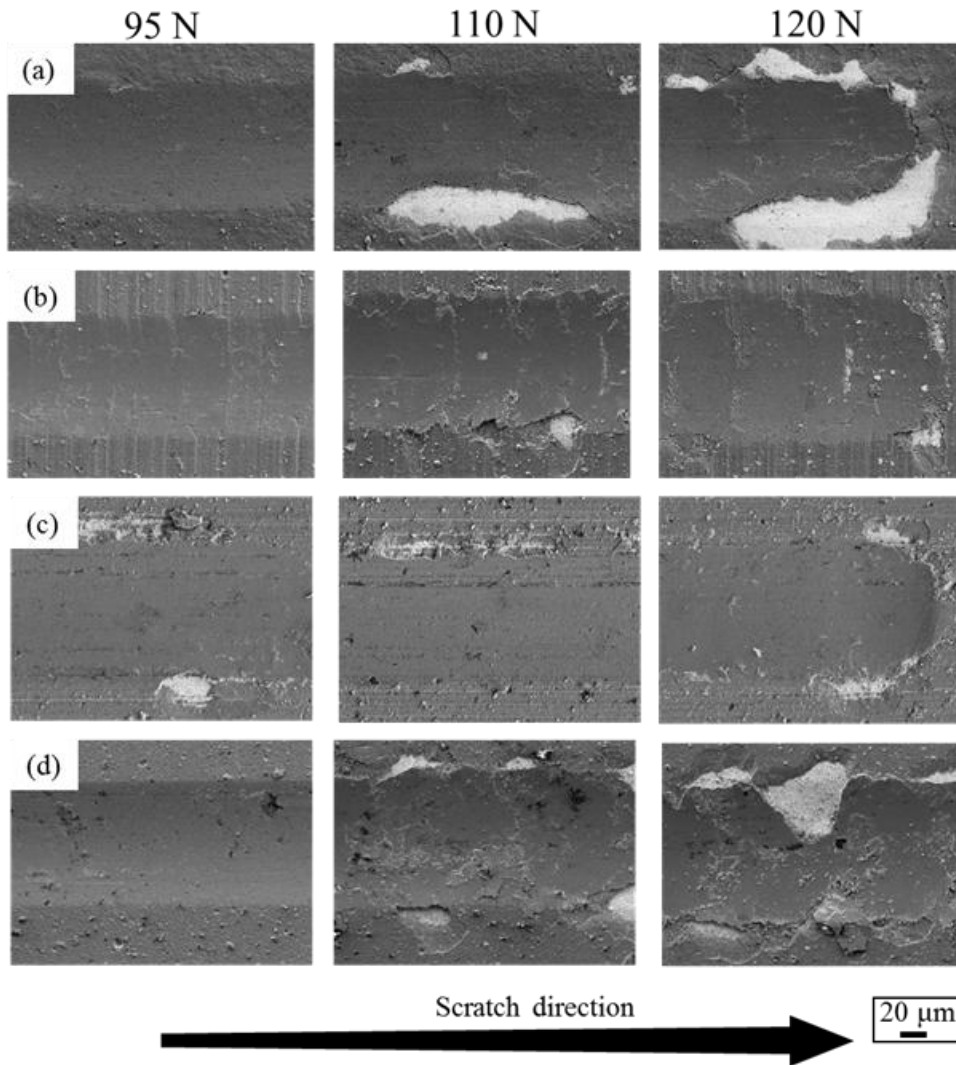
Fig. 4. Scratch track view associated with three different applied normal load levels: 95 N, 110 N and 120 N, for the coated systems with distinct surface finish conditions: (a) AS; (b) G-⊥; (c) G-// and (d) P. Scratch direction from left to right.

Figure 5.

Top view

Inclined view

(a)

10 μm

(b)

1 μm

(c)

10 μm

(d)

1 μm

(e)

10 μm

(f)

1 μm

(g)

10 μm

(h)

1 μm
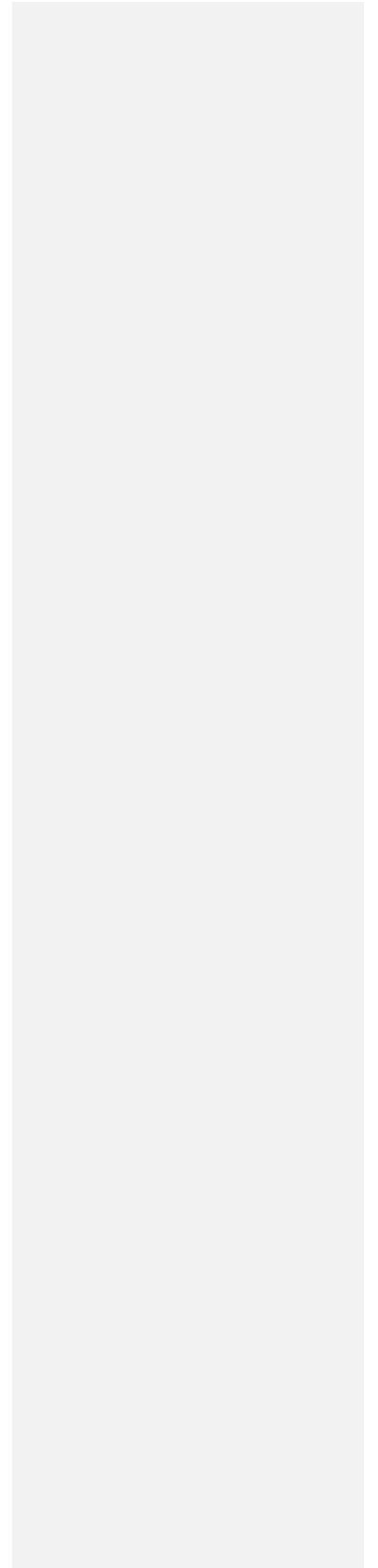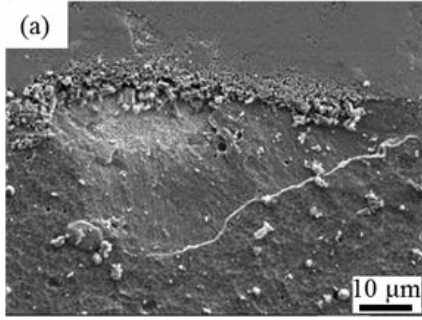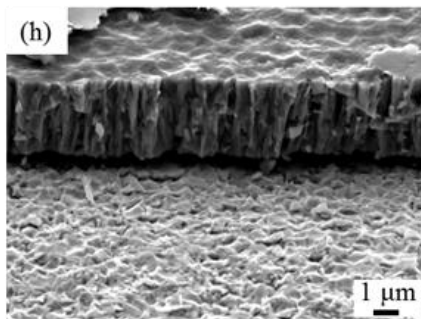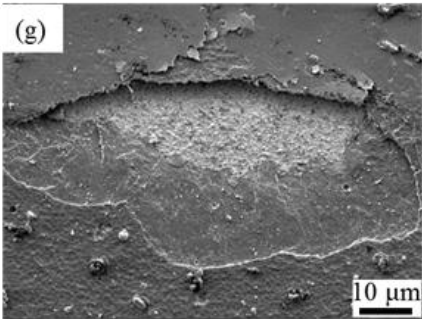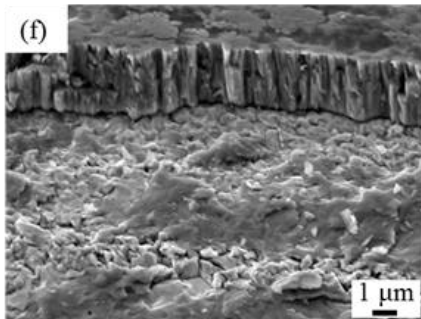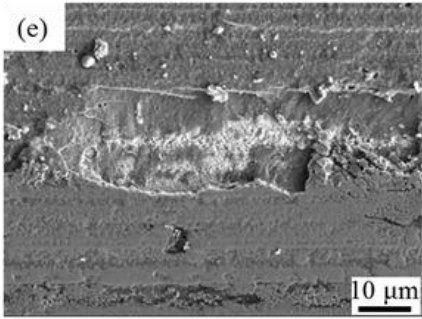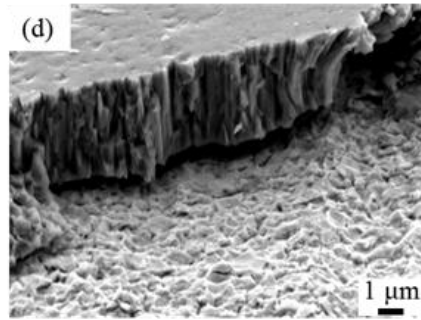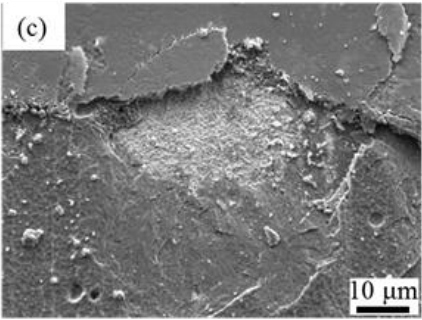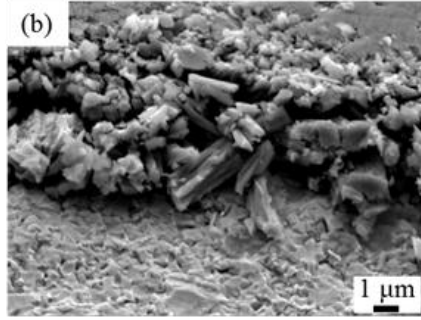
Fig. 5. Adhesive failure scenario for all the coated systems at scratch track position corresponding to critical normal load: (a, b) AS; (c, d) G-$\perp$; (e, f) G-// and (g, h) P. (a, c, e and g) are top view image, where (b, d, f and h) are inclined image at the rim of the spallation region.
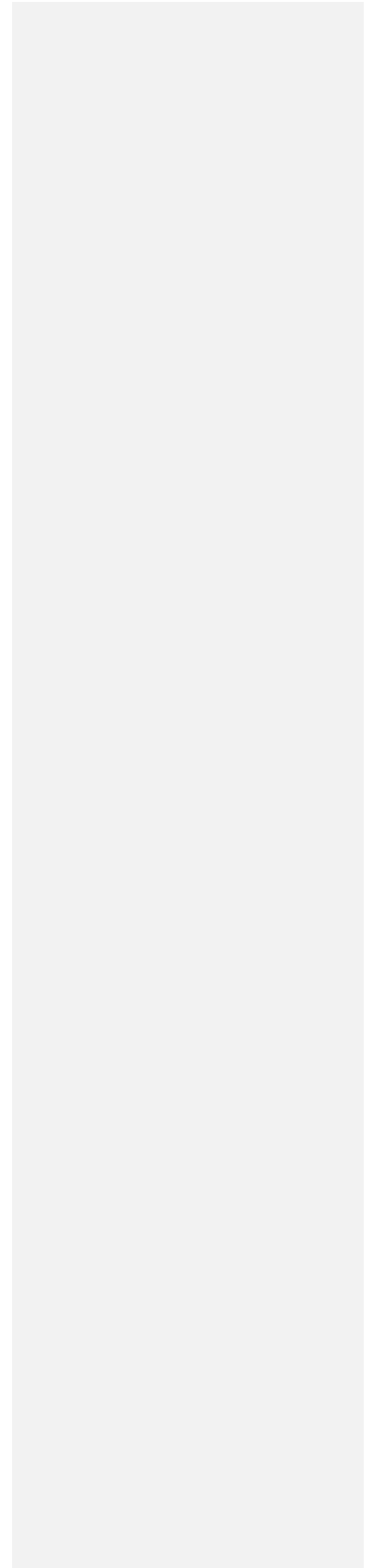
Figure 6.
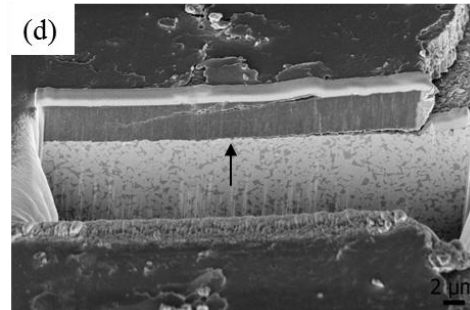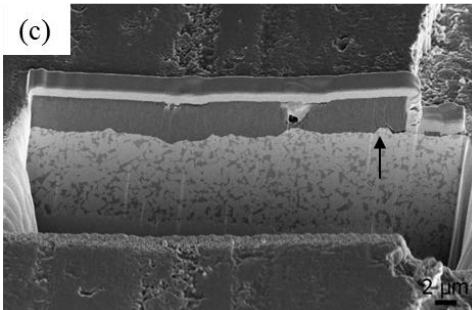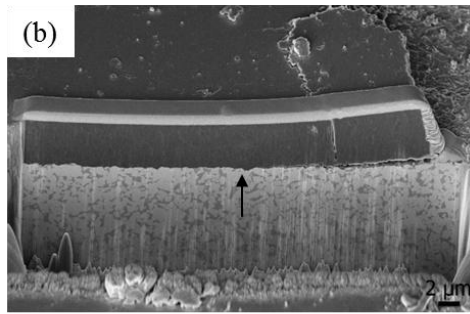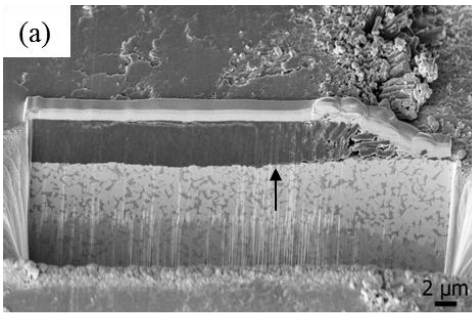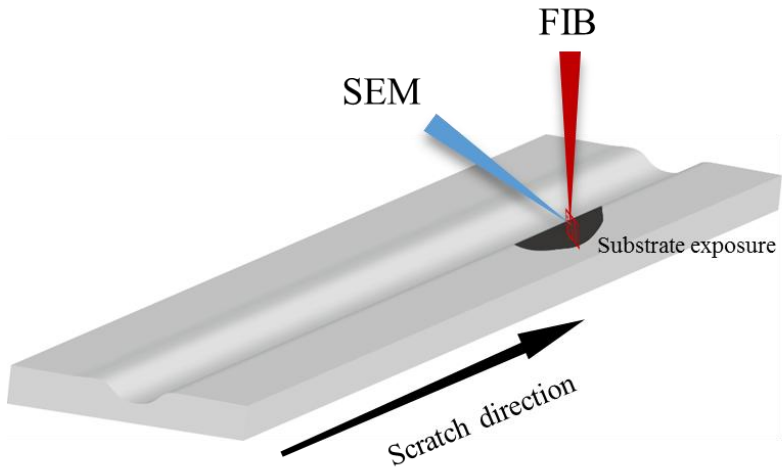
Fig. 6. FIB milled cross section and FESEM view of scratch track edges corresponding to the critical normal load for all the coated systems. The beginning of the interfacial crack is marked using arrows for each condition. (a) AS; (b) G-⊥; (c) G-// and (d) P.
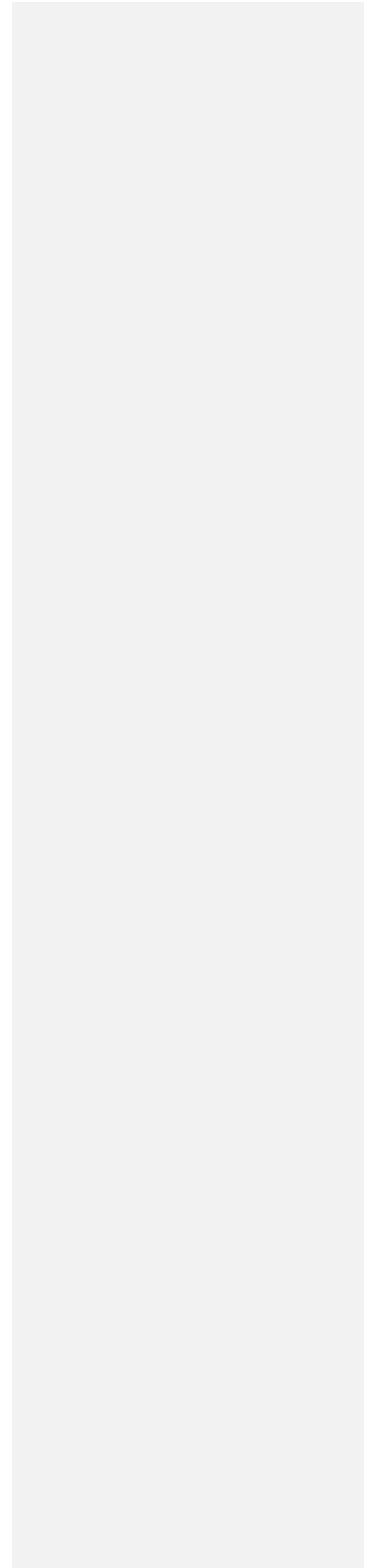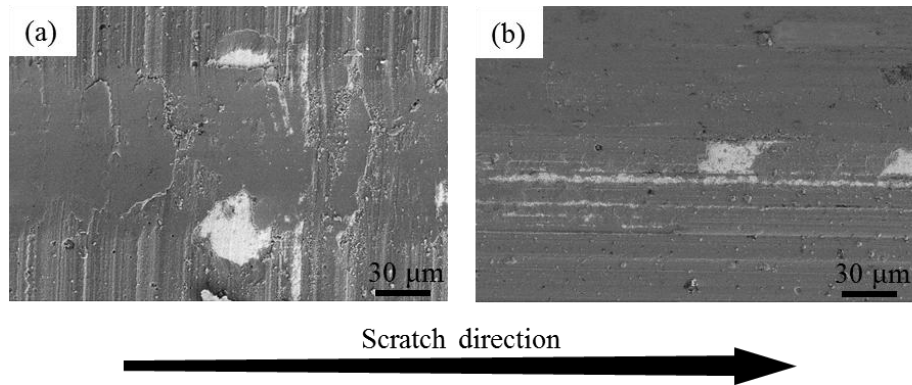
Figure 7.

Scratch direction

Fig. 7. Adhesive failure of the coated systems corresponding to heat-treated hardmetal substrates (prior to TiN coating) at applied L_c: (a) GTT-$\perp$, and (b) GTT-$/\!/$. Scratch direction from left to right.
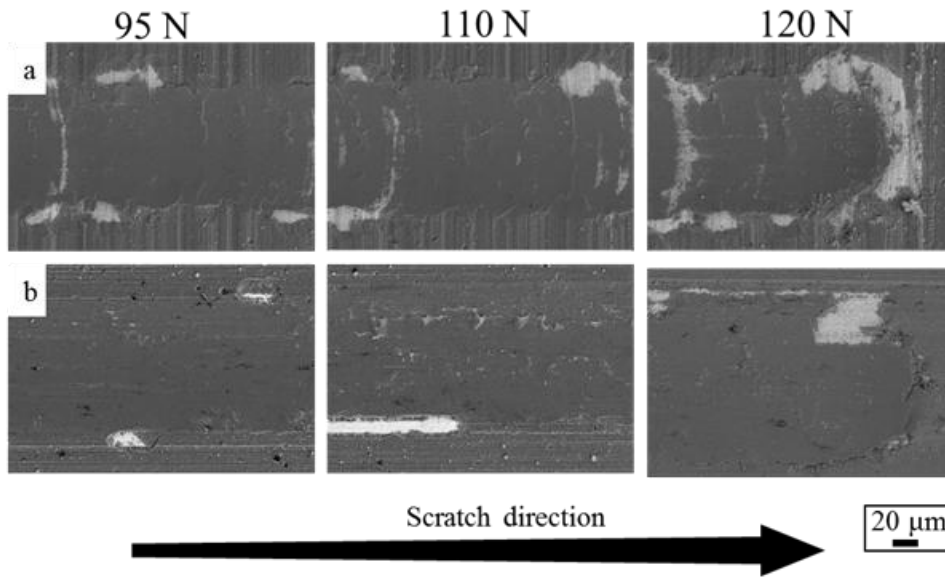
Figure 8.

Fig. 8. Scratch track view associated with three different applied normal load levels: 95 N, 110 N and 120 N for coated GTT systems with each row corresponding to surface finish conditions: (a) GTT-⊥; and (b) GTT-//. Scratch direction from left to right.
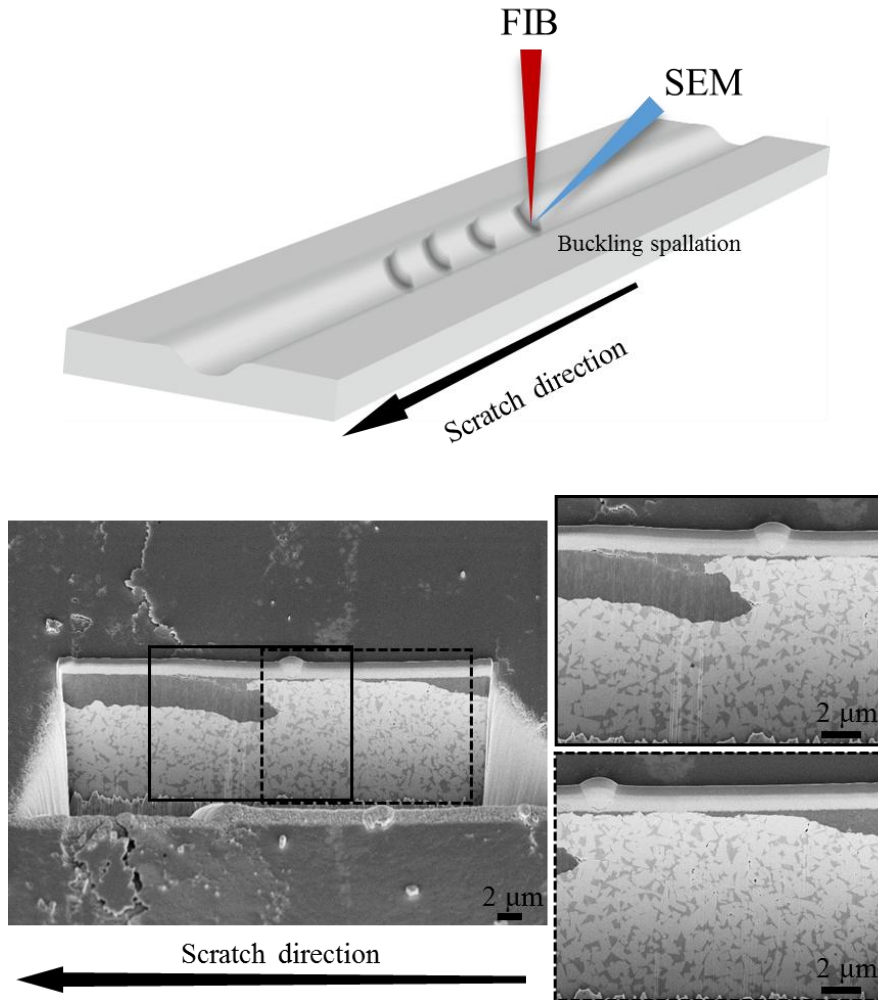
Figure 9.

Fig. 9. Longitudinal cross-section view of the GTT-⊥ coated system associated with the initial buckling spallation (at about 65 N) by means of FIB milling and SEM inspection. Scratch direction from right to left. The two images at the right are the enlarged views of the solid and dash squares indicated in the image at the left, respectively.
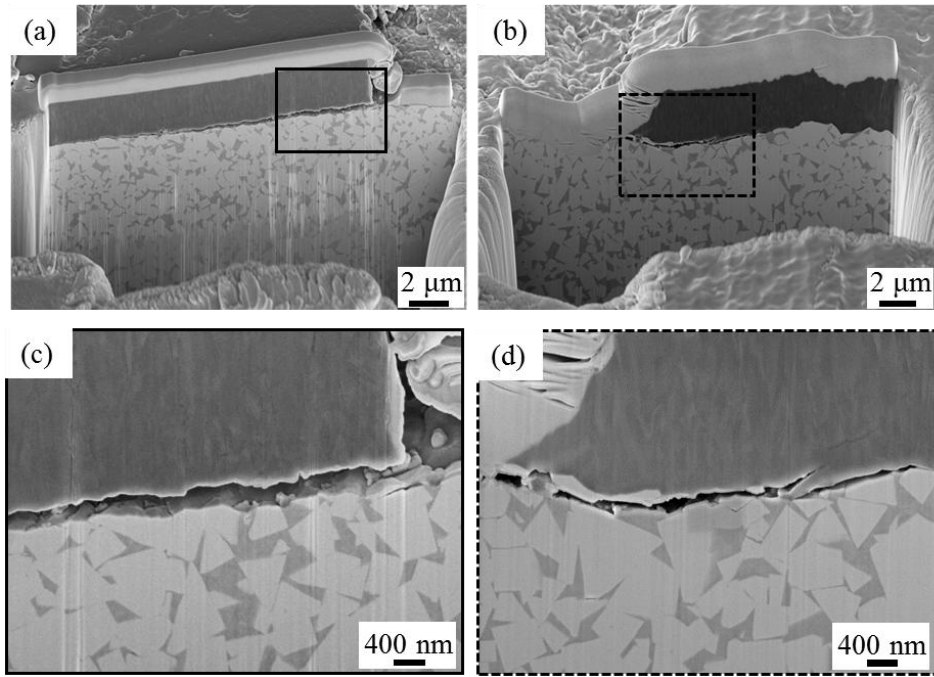
Figure 10.

Fig. 10. FIB milled cross section and FESEM view for the coated GTT systems at the scratch track edges corresponding to applied L_c: (a, c) GTT-⊥: and (b, d) GTT-//. (c) and (d) are the enlarged views of the squares indicated in (a) and (b), respectively.